Excitonic sensor of electric field in quantum-well heterostructures

M. A. Chukeev ◉, Sh. Zheng, E. S. Khramtsov ◉, and I. V. Ignatiev ◉

Spin Optics Laboratory, St. Petersburg State University, Ulyanovskaya 1, Peterhof, St. Petersburg, 198504, Russia

S. A. Eliseev, V. A. Lovtcius ◉, Yu. P. Efimov, and M. A. Lozhkin

Resource Center "Nanophotonics", St. Petersburg State University, Ulyanovskaya 1, Peterhof, St. Petersburg, 198504, Russia

We present an experimental and theoretical study of the lowest exciton states in a 30-nm single GaAs quantum-well heterostructure in different electric fields. We found that the excitons in quantum wells are highly sensitive to an electric field and demonstrate nonlinear behavior in terms of their energy position, amplitude, spectral width, and phase of exciton resonances in reflection spectra. Comparison of experimental results with theoretical calculations allowed us to reliably determine the electric field strength in the quantum-well layer.

I. INTRODUCTION

Excitons in the GaAs/AlGaAs heterostructures with quantum wells (QWs) are well-studied objects of both experimental and theoretical works [1–4]. High quality of GaAs/AlGaAs structures grown by molecular beam epitaxy (MBE) has been achieved [5–11]. Experimental methods make it possible to accurately determine parameters of exciton states [10,11]. Theoretical modeling allows one to calculate most exciton parameters with high accuracy [3,12–14]. This is the basis for the use of the exciton as a sensitive sensor of the electric field in QWs.

The effects of external electric fields on exciton states in QWs have been studied experimentally and theoretically for several decades (see, e.g., Refs. [15–23] and references therein). Several effects were observed in these studies. Already in the first works [15,24,25], the quantum-confined Stark effect in GaAs/AlGaAs structures was experimentally discovered and theoretically described. The effect manifests itself as an energy shift of exciton states when an electric field is applied along the growth axis of the structure. The shift of the heavy- and light-hole exciton states is experimentally demonstrated and its theoretical description is given.

Another effect of the electric field is a change in the oscillator strength of exciton transitions [16,26]. For the ground quantum-confined states of the heavy- and light-hole excitons, a decrease in the oscillator strength is observed. This is due to a decrease in the overlap of the wave functions of the electron and the hole in the exciton. However, for exciton transitions initially forbidden by symmetry, for example, for the transition between the second quantum-confined state and the ground (vacuum) state, an increase in the oscillator strength is observed. The increase is associated with the electric-field-induced lowering in the symmetry of the system [16,27,28].

The decrease in the oscillator strength of the ground states is accompanied by an increase in the lifetime of excitons. In high-quality heterostructures with coupled quantum wells, the exciton lifetime can reach microseconds when the

nonradiative losses are absent. This is many orders of magnitude longer than the radiation lifetime in the absence of the electric field (∼10 ps). This effect is used to observe the Bose-Einstein condensation of excitons and other collective effects in exciton systems [23,29–31].

The electric field also leads to the appearance of static dipole moment of excitons, which significantly affects their interaction with each other [21,32–35]. In the absence of the electric field, the main mechanism of exciton-exciton interaction is the exchange interaction [36–41]. With an increase in the electric field and, accordingly, the dipole moment of the exciton, the direct dipole-dipole interaction of excitons can prevail over their exchange interaction. In particular, this effect was used to increase the nonlinearities in the polariton system [21].

The polarization of the exciton in an electric field leads to a decrease of the Coulomb interaction between the electron and the hole in the exciton causing the reduction of the exciton binding energy [15,42,43]. In sufficiently strong electric fields, the potential barriers for the electrons and the holes in the QW decrease and become of finite width. The electron or the hole can tunnel through these barriers leading to exciton dissociation [42–44]. In other words, in addition to the radiative recombination, the exciton can decay into a free electron and a hole. This process leads to a reduction in the exciton lifetime in sufficiently strong fields and wide QWs. In experiments, this is observed as an additional homogeneous broadening of exciton transitions [45].

Free charge carriers may also be present in the heterostructure. For example, intentional or background doping of individual layers of the structure, as well as optical excitation with high photon energy, increases the charge-carrier concentration [5]. In this case, the application of an electric field can lead to the movement of the charge carriers, which causes partial or complete screening of the field in the QW under study [17,46,47]. As a result, the distribution of the electric field in the structure can be very inhomogeneous. The problem is further complicated by the complexity of the design of the

235305-1

structures typically studied in experiments. All these problems with uncontrollable doping of structure layers dramatically complicates the quantitative analysis of phenomena observed in electric fields, as it was noted in most of the works cited above. In this regard, independent control of the electric field strength in the layers of the structure is an important task.

In this paper, parameters of exciton resonances observed in the reflection spectra were experimentally and theoretically studied to understand the behavior of excitons in GaAs/AlGaAs QWs when an electric voltage is applied to the heterostructure. Additional optical excitation of the structure below the exciton transitions in QW, when light is absorbed only in the GaAs buffer layer, made it possible to detect an indirect effect of charge carriers generated in the layer on the behavior of exciton resonances in the QW. It was found that even when the structure is excited by the low-power radiation (few tens of microwatts within the laser spot of 150 μm in diameter), a nonlinear shift and broadening of exciton resonances are observed in the QW. A strong influence of the electric field on the second quantum-confined state of the heavy-hole exciton has also been found.

The main results were obtained by experimentally studying the reflection spectra and analyzing them within the framework of the nonlocal dielectric response model [3], which makes it possible to determine all the parameters of exciton resonances. To understand the effects observed in the electric field, a microscopic calculation of exciton states in QWs was performed for various electric field strengths. Comparison of experimental data with results of the theoretical calculations allowed us to obtain a self-consistent method for determining the electric field strength.

II. STUDIED STRUCTURE AND METHODS

The studied sample is a high-quality GaAs/AlGaAs heterostructure with a 30-nm QW grown by MBE on an *n*-doped GaAs:Si substrate. The structure of the sample is shown in Fig. 1(a). The barrier layers are the short-period AlAs/GaAs superlattices with an average aluminum concentration of 15%. The *n*-doped substrate and the barriers are separated by a thick GaAs buffer layer with the thickness of 900 nm. The total thickness of all undoped epitaxial layers is 1310 nm.

The electric field was created using a voltage applied along the growth axis of the structure. One of the contacts (the Ohmic contact) is the *n*-doped GaAs substrate, and the second one (the Shottky contact) is the indium tin oxide (ITO) layer. The electronic band structure is shown in Fig. 1(c).

In addition to the applied voltage, optical excitation into various spectral regions was used to control the electric field in the QW layer. In this work, we used the excitation into the exciton transition in the GaAs buffer layer ($\hbar\omega = 1.516$ eV). The QW layer is transparent for this excitation photon energy. However, as we found, the exciton in the QW is very sensitive to this excitation.

The experimental part of the work was performed using reflection spectroscopy. The simplified optical excitation scheme is shown in Fig. 1(b). The sample was cooled down to a temperature of 10 K in a closed-cycle cryostat. The spectra were recorded using a spectrometer with a diffraction grating of 1200 grooves/mm and a focal length of 550 mm. The
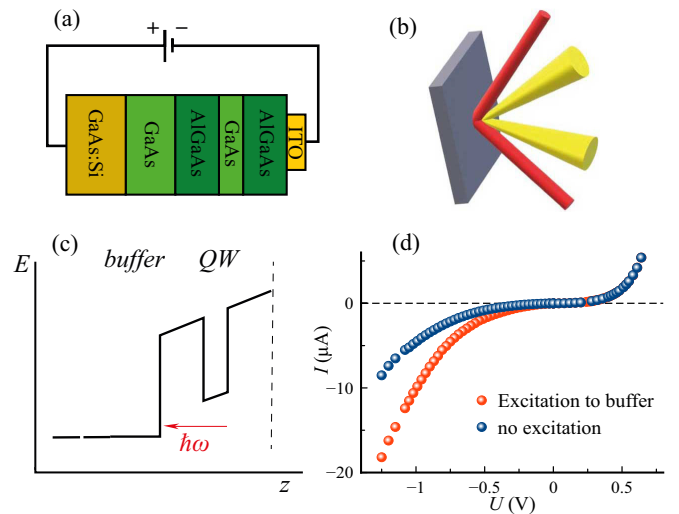

FIG. 1. (a) The block scheme of the studied sample, (b) the optical excitation scheme of the sample, (c) the electronic band heterostructure when a negative potential is applied to the sample surface, (d) the current-voltage characteristics of the sample in the presence of laser pumping (red symbols) and without it (blue symbols).

spectrometer is equipped with a matrix photodetector (CCD) cooled with liquid nitrogen. The reflection spectra were measured with a low-power continuous-wave light source (a halogen incandescent lamp) at the almost normal light incidence. To exclude undesirable excitation of states above the studied spectral region, the short-wave radiation of the lamp was cut off by a broadband optical filter. As an additional excitation, radiation from a tunable titanium-sapphire laser focused into a spot with a diameter of 120 μm was used.

For each measured spectrum, the current-voltage characteristics (CVC) were also measured. Examples of the CVC measured with or without of the laser excitation are shown in Fig. 1(d). Such a dependence of the current on the applied voltage corresponds to the diode CVC, namely, the Shottky diode was created by the contact semiconductor/ITO. However, there is a weak increase in the current when the negative potential is applied on the sample surface. A possible origin of this current is leakage through dislocations in the heterostructure. In this paper, we discuss only the effect of the electric field under the reverse (negative) bias.

III. EXCITON REFLECTION SPECTRA IN ELECTRIC FIELDS

Figure 2 shows the reflection spectrum of the investigated heterostructure under additional optical excitation below the exciton resonances in the QW. The experiment shows that, in the absence of voltage, the reflection spectrum is insensitive to the weak optical excitation ($P = 30$ μW). Three exciton resonances are observed in the spectrum. They correspond to the ground quantum-confined states of the heavy-hole (Xhh1) and light-hole (Xlh1) excitons and to the second quantum-confined state of the heavy-hole exciton (Xhh2). The shape of the exciton resonances is determined by the interference of light reflected from the sample surface and the QW layer
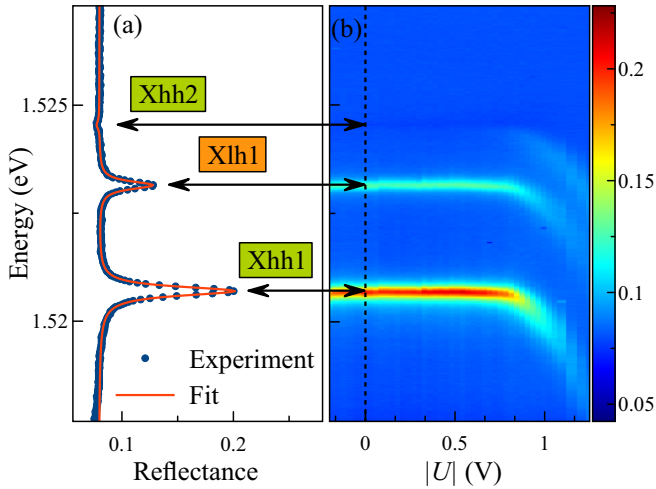
FIG. 2. (a) Exciton reflection spectrum measured under additional excitation with photon energy lower than the exciton transitions in the QW. The pumping power is of $P = 30$ μW. The arrows indicate the energies of exciton resonances in the absence of voltage. (b) Two-dimensional map of reflection spectra depending on the applied voltage.
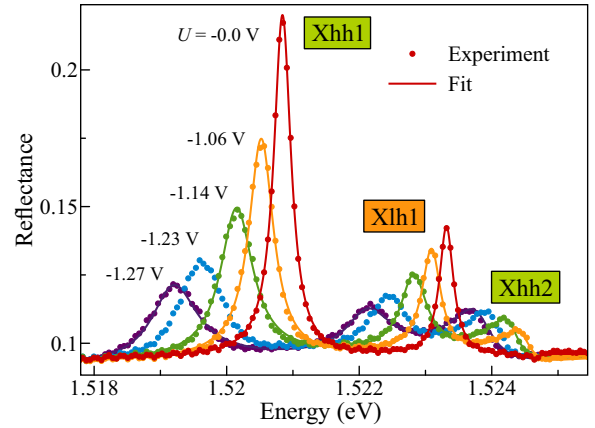

FIG. 3. Experimental reflection spectra measured at different voltages applied to the sample (symbols). Smooth curves represent the fit by formulas (1) and (2).

[10]. When growing the heterostructure under study, the thicknesses of the epitaxial layers (315 nm above the QW layer), as well as the ITO layer (100 nm), were chosen in a special way to obtain constructive interference of light reflected from the QW layer and the sample surface. In this case, the resonances of the lowest exciton states represent reflection peaks.

The exciton resonances are analyzed in the framework of the nonlocal optical response theory described in Ref. [3]. The amplitude reflection r_{QW} induced by exciton resonances in the QW is given by the expression

$$r_{QW} = \sum_j \frac{i(-1)^{(j-1)}\Gamma_{0j}e^{i2\phi_j}}{\omega_{0j} - \omega - i(\Gamma_j + \Gamma_{0j})}. \quad (1)$$

Here Γ_{0j} describes the radiative decay rate of the jth exciton state, Γ_j is the rate of the nonradiative relaxation from this state, and ω_{0j} is the frequency of the exciton transition j. The parameter ϕ_j describes the phase of the exciton resonance. It is the sum of the phase acquired by the light wave propagating from the sample surface to the QW layer and the phase related to the asymmetry of the QW potential [13]. These four quantities are used as fitting parameters of the model for each particular exciton resonance. The factor $(-1)^{(j-1)}$ in Eq. (1) takes into account the symmetry of exciton wave function for the odd ($j = 1, 3, \ldots$) and even ($j = 2, 4, \ldots$) quantum-confined exciton states, separately for the heavy- and light-hole excitons [8].

The total reflection also depends on the amplitude reflection coefficient of the sample surface r_s, and can be expressed as

$$R = \left| \frac{r_s + r_{QW}}{1 + r_s r_{QW}} \right|^2. \quad (2)$$

Figure 2(a) shows the result of fitting the reflection spectrum by Eqs. (1) and (2). As can be seen from the figure, the shape of the main exciton resonances is well described

by these formulas. This result allows us to determine the main parameters of the resonances. In particular, the radiative broadening $\hbar\Gamma_{0j}$ in the zero field turns out to be equal to 27 μeV Xhh1 state and 10 μeV for the Xlh1 state. The nonradiative broadening of both resonances is about 100 μeV. The Xhh1 phase $\phi = 0.06$ rad and the Xlh1 phase $\phi = 0.08$ rad. The accuracy of the obtained phase values is ± 0.02 rad. The Xhh2 state is almost invisible at zero voltage.

The effect of the negative potential applied to the sample surface on the exciton resonances is shown in Fig. 2(b). The figure shows a two-dimensional map of reflection spectra when an external voltage is applied. Nonlinear behavior is observed for all exciton resonances. Thus, at $|U| < 0.7$ V, the position of the resonances and their amplitude do not depend on the voltage. The application of a potential $|U| > 0.7$ V leads to a decrease in the amplitude and a shift of the main exciton resonances Xhh1 and Xlh1 towards lower energies. In the case of Xhh2, rapid increase in the amplitude and its shift to the low energy with a noticeable phase change is observed.

Exciton reflection spectra measured at different voltages are well modeled using formulas (1) and (2). Examples of the fitting are shown in Fig. 3. The good agreement of the experiment and the model spectra allows us to quantitatively analyze the effect of the electric field on all parameters of exciton resonances.

On the other hand, it is possible to theoretically describe the behavior of exciton states in an external electric field using a numerical solution of the three-dimensional Schrödinger equation [11–14]. Details of the calculations are described in the next section. The theoretically calculated reflection spectra are shown in Fig. 4. The theoretical spectra were calculated using Eqs. (1) and (2), where all exciton parameters, except the nonradiative broadening, were obtained from the microscopic calculations. The calculations do not contain any free parameters. The nonradiative broadening is assumed to be 100 μeV, which corresponds to that in the experimental spectra.

As seen in Fig. 4, the theoretical spectra reproduce well the behavior of exciton resonances observed experimentally (Fig. 3). At the same time, the calculations assume that the
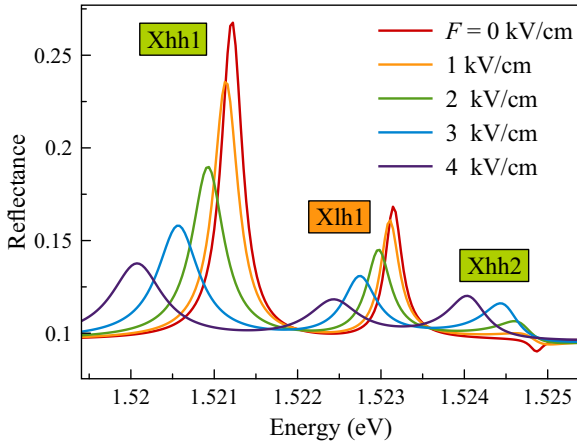
FIG. 4. Theoretically modeled reflection spectra in various electric fields.

TABLE I. Material parameters for GaAs/Al$_x$Ga$_{1-x}$As heterostructures [51].

	GaAs	AlAs
m_e	0.067	0.15
γ_1	6.98	3.76
γ_2	2.06	0.82
ε from Ref. [52]	12.53	10.06

electric field strength in the QW is close to zero at low voltages up to $|U| \approx 0.9$ V (see Fig. 2). The reasons why the electric field strength nonlinearly depends on the applied voltage will be discussed in Sec. VI A.

IV. MICROSCOPIC CALCULATION OF EXCITON STATES

The previously developed numerical method [12] allows us to find a solution to the Schrödinger equation for an exciton in a QW in an external electric field:

$$\left[-\frac{\hbar^2}{2\mu_{jhxy}} \left(\frac{\partial^2}{\partial \rho^2} - \frac{1}{\rho} \frac{\partial}{\partial \rho} + \frac{1}{\rho^2} \right) - \frac{\hbar^2}{2m_e} \frac{\partial^2}{\partial z_e^2} \right.$$
$$\left. - \frac{\hbar^2}{2m_{jhz}} \frac{\partial^2}{\partial z_h^2} + V \right] \chi(\rho, z_e, z_h) = E \chi(\rho, z_e, z_h), \quad (3)$$

where

$$V = V_e(z_e) + V_h(z_h) + eF(z_e - z_h) - \frac{e^2}{\varepsilon \sqrt{\rho^2 + (z_e - z_h)^2}}. \quad (4)$$

The first term in Eq. (3) is the kinetic energy operator of relative electron-hole motion in the exciton in the QW plane (along the x and y coordinates), where ρ is the distance between the electron and the hole and $\mu_{hxy} = m_e m_{hxy}/(m_e + m_{hxy})$ is the reduced mass of the exciton. The second and third terms are operators of the kinetic energy of the motion of the electron and the hole across the QW layer, where m_e and m_{hz} are, respectively, the effective masses of the electron and the hole along the z axis. We take into account the anisotropy of the hole effective mass $m_{hz} \neq m_{hxy}$, which is described by the Luttinger parameters [11,12,48].

The last term in Eq. (3) represents the potential energy given by Eq. (4). The rectangular potential of the QW is described by the terms V_e and V_h for electrons and holes, respectively. The next term describes the effect of an external electric field, where e is the electron charge. The last term in Eq. (4) describes the electron-hole Coulomb interaction, where ε is the dielectric constant of the medium. The function χ is defined as $\chi(\rho, z_e, z_h) = \rho \psi(\rho, z_e, z_h)$, where

$\psi(\rho, z_e, z_h)$ is the exciton wave function. The multiplier ρ is introduced to implement zero boundary conditions at the coinciding coordinates of the electron and the hole.

The numerical implementation of the calculations is based on the finite-difference method, in which the Schrödinger equation is represented in the matrix form [11,12,49]. To determine the exciton energies and the wave functions, the lowest eigenvalues and eigenvectors of the matrix are calculated. The error of approximation of the differential equation by finite differences decreases with a decreasing in the step of the grid used. In this work, the calculation region was 200 nm for each coordinate: ρ, z_e, and z_h. The grid step was successively reduced from 2 to about 0.9 nm, and then the result was extrapolated to the zero grid step.

The wave functions of exciton states obtained in the calculations make it possible to find the exciton-light coupling constants and the phases of exciton resonances. The constants $\hbar\Gamma_{0j}$ are calculated using the formula [3,50]

$$\hbar\Gamma_{0j} = \frac{2\pi q}{\varepsilon} \left(\frac{e|p_{cv}|}{m_0 \omega_{0j}} \right)^2 \left| \int_{-\infty}^{\infty} \Phi_j(z) \exp(iqz) \, dz \right|^2. \quad (5)$$

Here, $\Phi_j(z) \equiv \psi_j(z_e = z, z_h = z, \rho = 0)$ is the cross section of the exciton wave function $\psi_j(z)$ with coinciding coordinates of the electron and hole, $q = \sqrt{\varepsilon}\omega/c$ is the wave vector of the light wave, ω_{0j} is the exciton resonance frequency, p_{cv} is the matrix element of the momentum operator between the electron and hole states.

The exciton resonance phase $\phi_j(F)$ associated with the asymmetry of the exciton wave function in the electric field is given by the ratio of integrals [13]:

$$\tan\left(\frac{\phi_j(F)}{2} \right) = \frac{\int \Phi_j(z) \sin(qz) \, dz}{\int \Phi_j(z) \cos(qz) \, dz}. \quad (6)$$

Note that the total phase of the exciton resonance is the sum of the field-induced phase $\phi_j(F)$ and the phase acquired by light wave propagating to the QW [see comment to Eq. (1)]. The latter quantity can be easily calculated taking into account geometrical parameters of the heterostructure under study [10].

The material parameters used to calculate the exciton states are given in Table I. Other parameters are as follows. The offset of the band gaps for the GaAs and Al$_{0.15}$Ga$_{0.85}$As crystals, $\Delta E_g = 172.9$ meV [11]; the ratio of the offsets for conduction and valence bands, $V_e/V_h = 2$; $E_p = 2|p_{cv}|^2/m_0 = 28.8$ eV [51]. The anisotropic effective masses [48] (in units of free-electron mass) of the hole are $m_{hz} = 1/(\gamma_1 \mp 2\gamma_2)$ in the growth direction and $m_{hxy} = 1/(\gamma_1 \pm \gamma_2)$ in the QW plane. The upper sign refers to the heavy hole and the lower sign corresponds to the light hole. The linear interpolation between the corresponding values for the GaAs and AlAs is used to
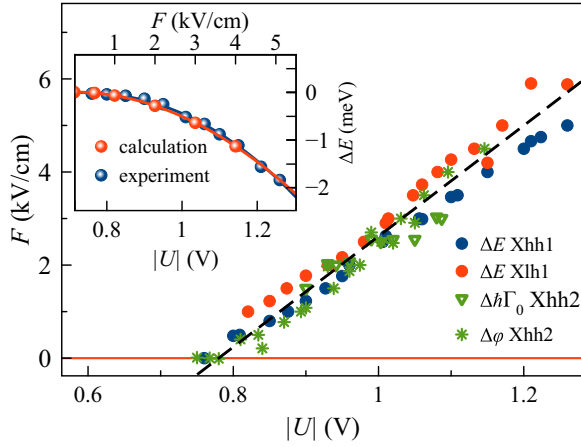
FIG. 5. Dependence of the electric field strength in the QW on the applied voltage determined using various parameters of exciton resonances (symbols). A solid line is a linear fit. The inset shows an example of the dependence of the Xhh1 exciton resonance shift found from the experiment (blue symbols) and calculated theoretically (red symbols). Solid curves are parabolic approximations.

obtain the dielectric constant ε and the effective masses of charged carriers for the $Al_{0.15}Ga_{0.85}As$ barrier layers.

In the theoretical modeling of exciton reflection spectra in an electric field, we used the exciton energy calculated by solving the Schrödinger equation (3), the exciton-light coupling constants determined by expression (5), and the phases determined by expression (6). The nonradiative broadening included in Eq. (2) cannot be obtained from the Schrödinger equation, therefore, it was extracted from experimental data.

The comparison of Fig. 3 (experiment) with Fig. 4 (simulation) clearly shows that the theoretically modeled reflection spectra describe well the electric-field-induced modification of exciton resonances Xhh1, Xlh1, and Xhh2 in the experiment. The high accuracy of microscopic calculations and the good agreement of the phenomenological fit by formulas (1) and (2) with experimental data allows us to use excitons as sensitive probes of the electric field in QW.

V. EXCITONIC SENSOR

The data shown in Figs. 3 and 4 show that the electric field strength in the QW and the voltage applied to the heterostructure are nonlinearly related to each other. A detailed discussion of the physical mechanisms leading to this nonlinearity will be given below in Sec. VI. Here we use exciton parameters such as the exciton transition energy, the radiative broadening, and the resonance phase to determine a relationship between the applied voltage and the field strength in the QW. The inset in Fig. 5 shows the experimentally obtained dependence of the energy shift ΔE of the Xhh1 resonance as a function of the applied voltage (blue symbols, lower axis). As seen, this dependence is well approximated by a parabolic curve. The theoretical dependence of ΔE on the electric field strength (red symbols and curve, upper axis) is also shown here. As seen, both dependencies are close to each other in the selected range of applied voltages. This allows us to link
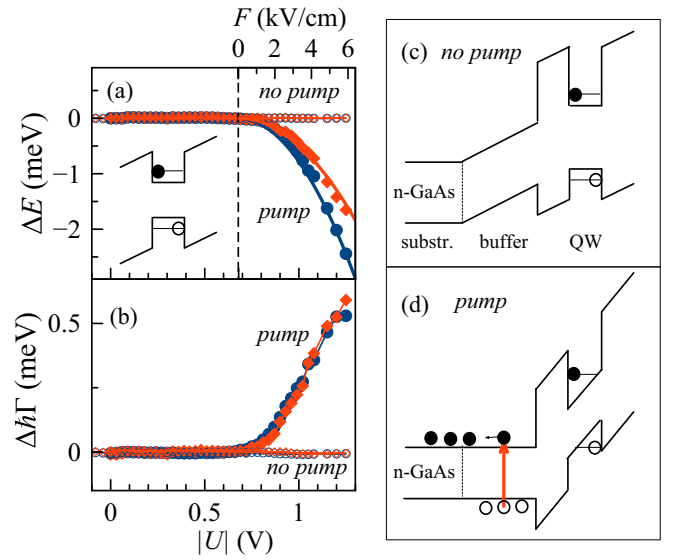

FIG. 6. Energy shift (a) and broadening of resonances (b) of the heavy-hole (blue symbols) and light-hole (red symbols) excitons as functions of applied voltage when there is no optical excitation (open symbols) and when the buffer layer is pumped (solid symbols). $P_{exc} = 30\,\mu W$. The solid curves on (a) show the theoretical dependencies of the shift of the resonances Xhh1 and Xlh1 on the electric field (upper scale). The insert on (a) illustrates the compensation of the electric field in the QW. (c), (d) Illustrate the change in the potential profile when the pumping is turned on.

the voltage applied to the heterostructure and the electric field strength in the QW.

Figure 5 shows the relationship between the electric field strength in the QW and the applied voltage, which was found using several exciton parameters. It can be seen that all parameters give approximately the same relationship, well approximated by a linear dependence in the voltage range 0.8–1.25 V. Thus, the exciton can really serve as a sensitive probe of the electric field strength in QWs. It should be noted that Xhh2 and Xlh1 exciton parameters are less reliably determined from the experiment. As seen in Fig. 3, the resonances are broadened at high voltages and they partially overlap each other. This results in the increase of errors in determining the radiative broadening and phase of resonances. The behavior of these resonances is discussed in the next section.

VI. EXCITON PARAMETERS

A. Lowest exciton states Xhh1 and Xlh1

The established relationship between the applied voltage and the electric field strength allows us to discuss the field dependencies of all parameters of exciton resonances. First, we discuss the shift ΔE and the nonradiative broadening $\hbar\Gamma$ of the exciton resonances Xhh1 and Xlh1. The radiative broadening and phases of these resonances are discussed in Sec. VI C. Figure 6 shows the dependencies of ΔE and $\hbar\Gamma$ on the applied voltage measured in two regimes: (i) in the absence of additional optical excitation (no pump) and (ii) when the pump excites the exciton transition in the buffer layer (pump).

In the absence of pumping, there is no noticeable energy shift or broadening of exciton resonances over the entire range of applied voltages. At the same time, the field strength, that could be created by the applied voltage and the potential of the Schottky barrier ($U_{Sh} \approx 0.6$ V, see Fig. 1) on the ITO/GaAs interface, is quite large. It is determined by the expression

$$F = \frac{U_{Sh} + |U|}{\varepsilon L}, \tag{7}$$

where the dielectric constant $\varepsilon = 12.53$ [52]. The maximum value of the applied voltage in the experiment is $|U|_{max} = 1.2$ V (see Fig. 6). The total thickness of the undoped epitaxial layer in the studied heterostructure is $L = 1.3$ μm. Hence, the maximum field strength $F_{max} = 1.1$ kV/cm. Theoretical calculations show (see Sec. IV) that, in such a field, the exciton resonances Xhh1 and Xlh1 should shift by the value $\Delta E \approx -0.1$ meV. This value is considerably greater than the experimental error in determining the exciton resonance energy ($\delta E \leqslant 0.015$ meV).

The absence of a noticeable exciton resonance shift (in the absence of pumping) means that the electric field is screened in the QW. The screening mechanism is associated with the presence of a small density of free electrons and holes. The electrons and holes are shifted to the opposite walls of the QW under the action of an applied voltage, and, thereby, compensate for the created electric field. This is schematically shown in the inset of Fig. 6(a). Free charge carriers can exist in the QW due to background doping, which is inevitably present in the heterostructure. Simple estimates show [53] that the free charge-carrier density sufficient for the electric field screening is $n_{ch} = 6 \times 10^{13}$ cm^{-3}. This value is small and is quite achievable due to background doping even in the high-quality heterostructures [5]. It is quite possible that the concentration of free charge carriers in the QW is even higher than the average for the heterostructure since some charge carriers can be captured from the nearest barrier layers.

In the thick GaAs buffer layer, complete compensation of the electric field apparently does not occur (otherwise it would have been observed in the experiment) due to the peculiarities of the background doping in the heterostructure under study. The analysis shows that our structure is *p* doped (carbon acceptors). The binding energy of the holes at the acceptor levels is quite high (≈ 30 meV), so they are inactive in such electric fields. A detailed discussion of this issue is given in Ref. [53].

Additional optical excitation into the exciton transition in the buffer layer generates excitons and free charge carriers in this layer. Unlike background charge carriers, photogenerated charge carriers are very mobile and easily separated by applied voltage. Excitons are also easily ionized by this voltage. The radiative lifetime of the free charge carriers increases dramatically as the overlap of the wave functions of electrons and holes decreases. In the extreme case, the lifetime is limited only by the nonradiative processes and reaches tens of nanoseconds in the studied structures [54,55]. This leads to accumulation of photocreated charge carriers in the buffer layer. An estimate of their concentration at a relatively weak optical excitation power, $P = 30$ μW in a spot with a diameter of 100 μm, shows [53] that the concentration of free carriers in the buffer layer can reach the value $n_{buf} = 8 \times 10^{13}$ cm^{-3}.

Such a concentration of carriers is sufficient to completely screen the electric field in the buffer layer. This is schematically shown in Figs. 6(c) and 6(d). As a result, the voltage is applied only to the layer consisting of barriers and the QW with total thickness of $L_{eff} = 0.41$ μm. The electric field strength increases sharply leading to a significant energy shift of exciton resonances. Experiments show that the used pumping power, $P = 30$ μW, is close to the minimum value when this effect is observed. With an increase in the pumping power, the magnitude of the shift of the resonances Xhh1 and Xlh1 increases slightly, still the dependence on the applied voltage remains similar [53].

Simultaneously, with the Stark shift of exciton resonances, a sharp increase in their nonradiative broadening is observed [see Fig. 6(b)]. This indicates an increase in the interaction of excitons with other quasiparticles and/or the exciton ionization in the QW. In principle, this could be a dipole-dipole interaction of excitons polarized by the electric field. However, theoretical estimates show that the magnitude of the exciton dipole moment is negligible. The two-dimensional density of excitons in the QW created by the probing light is also small. So, this effect is extremely unlikely in our experiments.

We assume that the nonradiative broadening is likely to increase as a result of ionization of a fraction of photogenerated excitons. The ionization reduces the exciton lifetime and, hence, increases the broadening. In addition, free charge carriers are created in the QW. The interaction of excitons with the charge carriers also results in the broadening of exciton resonances. This conclusion is consistent with the theoretical analysis performed in [41].

B. Excited state Xhh2

The behavior of the second quantum-confined state of the heavy-hole exciton, Xhh2, in an electric field requires a separate discussion. In the absence of the field, this state is hardly visible as a dip in the reflection spectrum. The small amplitude of the resonance is a typical feature of narrow QWs ($L_{QW} \ll \lambda$) and it is explained by the fact that the cross section $\Phi(z)$ of the wave function of this state is an odd function with respect to the symmetry operation $z \to -z$. Accordingly, the overlap integral with the light-wave component $E(z) = E_0 \cos(qz)$, included in expression (5) for the radiative broadening, is small. The overlap integral with another component, $E(z) = E_0 \sin(qz)$, is near to zero due to the relatively small width of the QW [14]. As a result, the exciton-light coupling is small for this state. The phase of this resonance is close to π due to the odd symmetry of function $\Phi(z)$ [see Eq. (6)]. This explains the appearance of the resonance as a dip in the reflection spectrum at zero electric field.

When an electric field is applied, the magnitude of the resonance increases dramatically and all parameters of the resonance are changed. Figure 7(a) illustrates the transformation of the experimentally observed Xhh2 resonance. Microscopic calculation makes it possible to well reproduce this transformation [see Fig. 7(b)]. Note that no fitting parameters were used in the calculations of exciton parameters. To model the reflection spectra in various electric fields we used some parameters found from the experiment: the nonradiative
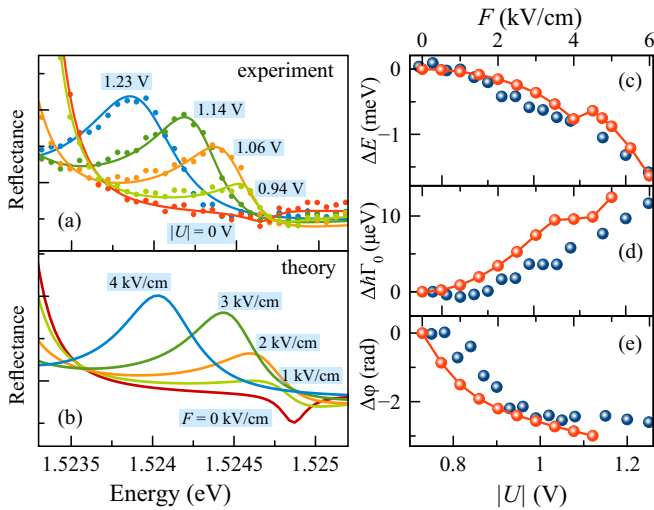
FIG. 7. Comparison of the experimental (a) and numerically modeled (b) behavior of the exciton resonance Xhh2 in an electric field. (c)–(e) Show the field dependencies of the energy shift, the radiative broadening, and the phase of the resonance, respectively, found from experiment (blue symbols) and microscopic calculation (red symbols and lines).

broadening, background reflectance, and phase of the resonance in zero field.

Similar to other exciton states, the Xhh2 state shifts to the lower energies [see Fig. 7(c)]. The application of the electric field also leads to a significant increase in the exciton-light coupling (the parameter $\hbar\Gamma_0$) [see Fig. 7(d)]. Finally, the electric field strongly changes the phase of this resonance [see Fig. 7(e)]. The physical origin of the strong change in the exciton-light coupling and the phase of this resonance, as well as a weak change in similar parameters of the Xhh1 and Xlh1 resonances, are discussed in the next section.

C. Radiative broadening and phases of exciton resonances

In addition to the shift and broadening of exciton resonances, the electric field leads to more subtle effects. In this section, we discuss the changes of the phase and the radiative broadening of exciton resonances Xhh1 and Xlh1. The theoretical and experimental behavior of these parameters is shown in Fig. 8. The experiment shows a small decrease in the phase of the Xhh1 resonance of about -0.25 rad at the maximum used voltage value $|U| = 1.2$ V (the field strength $F = 5$ kV/cm) [see Fig. 8(a)]. The theoretical calculation of the phase carried out using Eq. (6) also predicts a small decrease in the phase of this resonance, which is in good agreement with the experiment within the experimental errors.

For the Xlh1 resonance, the phase change observed in the experiment is small and comparable to the error of its determination. The relatively large error is caused by the mixing of the Xlh1 and Xhh2 exciton states (see Fig. 3). Theoretical calculation gives a small change in the phase of this resonance, which is qualitatively consistent with the experiment.

The radiative broadening of the Xhh1 state is reduced by a factor of 2 with increasing electric field up to $F = 5$ kV/cm, as observed in the experiment and reproduced by the theory
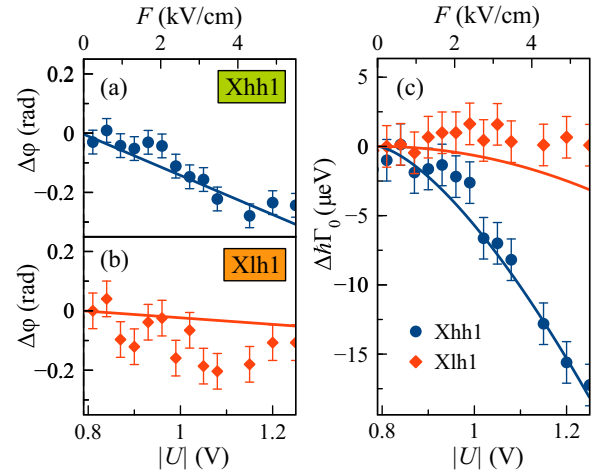

FIG. 8. Comparison of exciton parameters $\Delta\phi$ (a), (b) and $\hbar\Gamma_0$ (c) measured experimentally (symbols) and calculated (smooth curves). Dependencies for the Xhh1 state are highlighted in blue, and dependencies for the Xlh1 state are highlighted in red.

[see Fig. 8(c)]. On the contrary, the radiative broadening of the Xlh1 state is less sensitive to the electric field, and it does not change within the experimental errors. At the same time, the calculation predicts a small decrease in this exciton parameter. Such a discrepancy may also be due to the mixing of the Xlh1 and Xhh2 states. This is not taken into account in theoretical calculations.

The behavior of the exciton parameters $\hbar\Gamma_0$ and $\Delta\phi$ demonstrated in Figs. 7 and 8 can be understood by analyzing the behavior of the function $\Phi(z) \equiv \psi(z_e = z_h = z, \rho = 0)$. Figure 9 shows the $\Phi(z)$ functions for all three studied exciton states. The states Xhh1 and Xlh1 are characterized by a decrease in the integral of the function $\Phi(z)$ (see colored area) with an increase in the field strength. This fact explains the decrease of $\hbar\Gamma_0$ [see formula (5)].
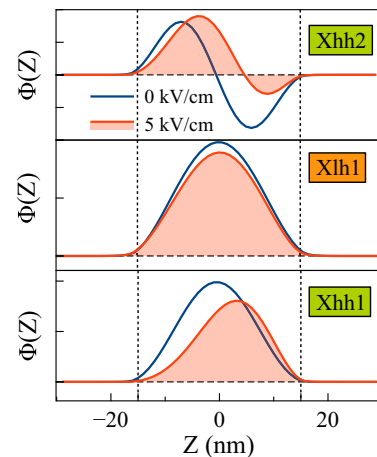

FIG. 9. Microscopically calculated functions $\Phi(z)$ for states Xhh1, Xlh1, and Xhh2 at the electric field $F = 0$ (blue curves) and $F = 5$ kV/cm (red curves). The shaded areas under the red curves show the integrals included in the expression (5) for the exciton-light coupling constant $\hbar\Gamma_0$.

For the Xhh2 state, the situation is qualitatively different. As can be seen from Fig. 9, the function $\Phi(z)$ has a sinelike form (blue curve) and the integral of this function is zero when $F = 0$. In an external electric field, the wave function becomes asymmetric and its integral (the shaded area) is nonzero. Due to this fact, the Xhh2 state becomes optically active in the specified range of electric fields. The asymmetry of function $\Phi(z)$ is also responsible for strong change of phase of this resonance [see Fig. 7(e)]. Indeed, according to Eq. (6), the phase is approaching to zero at large electric field because the denominator in this equation becomes large. So, the phase of the Xhh2 resonance changes from initial value π at zero electric field to almost zero at $F = 5$ kV/cm.

VII. CONCLUSION

We have performed an experimental and theoretical study of excitons in a GaAs/AlGaAs QW structure in an external electric field. High sensitivity of exciton resonances observed in reflection spectra allowed us to determine the magnitude of the electric field. Several parameters of the resonances, the energy position, the radiative broadening, and the phase of resonances, can be used for this purpose. To quantitatively determine the electric field strength, we have compared the experimental data with the results of microscopic calculations of exciton states in the structure under study. All parameters (except the nonradiative broadening) of exciton resonances give a consistent value of the field strength and its dependence on the voltage applied to the heterostructure. This consistence

is due to the high quality of the sample studied. The obtained results convincingly show that excitons can serve as a sensitive sensor of electric field.

It is found that the electric field strength nonlinearly depends on the voltage applied to the heterostructure. This is a result of the presence of a small concentration of free charge carriers due to the inevitable background doping of the heterostructure. When a small voltage is applied, $|U| < 0.8$ V, the movement of charge carriers in the quantum-well layer screens the electric field in this layer. Screening the electric field in other layers can, on the contrary, increase the field in the quantum-well layer. This conclusion is confirmed by the photocreation of a small concentration of free charge carriers in the buffer layer of the heterostructure. Experiments show that the electric field strength in the quantum well increases at least by an order of magnitude when the applied voltage increases from 0.8 to 1.25 V.

[1] R. Dingle, W. Wiegmann, and C. H. Henry, Quantum states of confined carriers in very thin $Al_xGa_{1-x}As$-GaAs-$Al_xGa_{1-x}As$ heterostructures, Phys. Rev. Lett. **33**, 827 (1974).

[2] B. Deveaud, F. Clérot, N. Roy, K. Satzke, B. Sermage, and D. S. Katzer, Enhanced radiative recombination of free excitons in GaAs quantum wells, Phys. Rev. Lett. **67**, 2355 (1991).

[3] E. L. Ivchenko, *Optical Spectroscopy of Semiconductor Nanostructures* (Alpha Science International, Ltd, Oxford, 2005).

[4] A. V. Kavokin, J. J. Baumberg, G. Malpuech, and F. P. Laussy, *Microcavities* (Oxford University Press, Oxford, 2017).

[5] M. J. Manfra, Molecular beam epitaxy of ultra-high-quality AlGaAs/GaAs heterostructures: Enabling physics in low-dimensional electronic systems, Annu. Rev. Condens. Matter Phys. **5**, 347 (2014).

[6] A. N. Poddubny, A. V. Poshakinskiy, B. Jusserand, and A. Lemaitre, Resonant brillouin scattering of excitonic polaritons in multiple-quantum-well structures, Phys. Rev. B **89**, 235313 (2014).

[7] S. Poltavtsev, Y. Efimov, Y. Dolgikh, S. Eliseev, V. Petrov, and V. Ovsyankin, Extremely low inhomogeneous broadening of exciton lines in shallow (In,Ga)As/GaAs quantum wells, Solid State Commun. **199**, 47 (2014).

[8] A. V. Trifonov, S. N. Korotan, A. S. Kurdyubov, I. Y. Gerlovin, I. V. Ignatiev, Y. P. Efimov, S. A. Eliseev, V. V. Petrov, Y. K. Dolgikh, V. V. Ovsyankin, and A. V. Kavokin, Nontrivial relaxation dynamics of excitons in high-quality InGaAs/GaAs quantum wells, Phys. Rev. B **91**, 115307 (2015).

[9] A. V. Trifonov, E. S. Khramtsov, K. V. Kavokin, I. V. Ignatiev, A. V. Kavokin, Y. P. Efimov, S. A. Eliseev, P. Y. Shapochkin, and M. Bayer, Nanosecond spin coherence time of nonradiative excitons in GaAs/AlGaAs quantum wells, Phys. Rev. Lett. **122**, 147401 (2019).

[10] P. Y. Shapochkin, S. A. Eliseev, V. A. Lovtcius, Y. P. Efimov, P. S. Grigoryev, E. S. Khramtsov, and I. V. Ignatiev, Excitonic probe for characterization of high-quality quantum-well heterostructures, Phys. Rev. Appl. **12**, 034034 (2019).

[11] M. N. Bataev, M. A. Chukeev, M. M. Sharipova, P. A. Belov, P. S. Grigoryev, E. S. Khramtsov, I. V. Ignatiev, S. A. Eliseev, V. A. Lovtcius, and Y. P. Efimov, Heavy-hole–light-hole exciton system in GaAs/AlGaAs quantum wells, Phys. Rev. B **106**, 085407 (2022).

[12] E. S. Khramtsov, P. A. Belov, P. S. Grigoryev, I. V. Ignatiev, S. Y. Verbin, Y. P. Efimov, S. A. Eliseev, V. A. Lovtcius, V. V. Petrov, and S. L. Yakovlev, Radiative decay rate of excitons in square quantum wells: Microscopic modeling and experiment, J. Appl. Phys. **119**, 184301 (2016).

[13] P. Grigoryev, A. Kurdyubov, M. Kuznetsova, I. Ignatiev, Y. Efimov, S. Eliseev, V. Petrov, V. Lovtcius, and P. Shapochkin, Excitons in asymmetric quantum wells, Superlattices Microstruct. **97**, 452 (2016).

[14] E. S. Khramtsov, P. S. Grigoryev, D. K. Loginov, I. V. Ignatiev, Y. P. Efimov, S. A. Eliseev, P. Y. Shapochkin, E. L. Ivchenko, and M. Bayer, Exciton spectroscopy of optical reflection from wide quantum wells, Phys. Rev. B **99**, 035431 (2019).

[15] D. A. B. Miller, D. S. Chemla, T. C. Damen, A. C. Gossard, W. Wiegmann, T. H. Wood, and C. A. Burrus, Band-edge electroabsorption in quantum well structures: The quantum-confined Stark effect, Phys. Rev. Lett. **53**, 2173 (1984).

[16] M. Matsuura and T. Kamizato, Subbands and excitons in a quantum well in an electric field, Phys. Rev. B **33**, 8385 (1986).

[17] S. Fafard, E. Fortin, and J. L. Merz, Excitation-intensity-dependent photoluminescence quenching due to electric-field screening by photocarriers captured in single-quantum-well structures, Phys. Rev. B **48**, 11062 (1993).

[18] A. V. Gorbunov and V. B. Timofeev, Large-scale coherence of the Bose condensate of spatially indirect excitons, JETP Lett. **84**, 329 (2006).

[19] A. V. Gorbunov, V. B. Timofeev, and D. A. Demin, Electro-optical trap for dipolar excitons in a GaAs/AlAs Schottky diode with a single quantum well, JETP Lett. **94**, 800 (2012).

[20] C. J. Dorow, M. W. Hasling, D. J. Choksy, J. R. Leonard, L. V. Butov, K. W. West, and L. N. Pfeiffer, High-mobility indirect excitons in wide single quantum well, Appl. Phys. Lett. **113**, 212102 (2018).

[21] S. I. Tsintzos, A. Tzimis, G. Stavrinidis, A. Trifonov, Z. Hatzopoulos, J. J. Baumberg, H. Ohadi, and P. G. Savvidis, Electrical tuning of nonlinearities in exciton-polariton condensates, Phys. Rev. Lett. **121**, 037401 (2018).

[22] D. K. Loginov, P. A. Belov, V. G. Davydov, I. Y. Gerlovin, I. V. Ignatiev, A. V. Kavokin, and Y. Masumoto, Exciton-polariton interference controlled by electric field, Phys. Rev. Res. **2**, 033510 (2020).

[23] D. J. Choksy, E. A. Szwed, L. V. Butov, K. W. Baldwin, and L. N. Pfeiffer, Fermi edge singularity in neutral electron–hole system, Nat. Phys. **19**, 1275 (2023).

[24] D. A. B. Miller, D. S. Chemla, T. C. Damen, A. C. Gossard, W. Wiegmann, T. H. Wood, and C. A. Burrus, Electric field dependence of optical absorption near the band gap of quantum-well structures, Phys. Rev. B **32**, 1043 (1985).

[25] C. Alibert, S. Gaillard, J. Brum, G. Bastard, P. Frijlink, and M. Erman, Measurements of electric-field-induced energy-level shifts in GaAs single-quantum-wells using electroreflectance, Solid State Commun. **53**, 457 (1985).

[26] E. E. Mendez, G. Bastard, L. L. Chang, L. Esaki, H. Morkoc, and R. Fischer, Effect of an electric field on the luminescence of GaAs quantum wells, Phys. Rev. B **26**, 7101 (1982).

[27] H. Iwamura, T. Saku, and H. Okamoto, Optical absorption of GaAs-AlGaAs superlattice under electric field, Jpn. J. Appl. Phys. **24**, 104 (1985).

[28] A. N. Pikhtin, O. S. Komkov, and K. V. Bazarov, Effect of external electric field on the probability of optical transitions in InGaAs/GaAs quantum wells, Semiconductors **40**, 592 (2006).

[29] L. V. Butov, C. W. Lai, A. L. Ivanov, A. C. Gossard, and D. S. Chemla, Towards Bose–Einstein condensation of excitons in potential traps, Nature (London) **417**, 47 (2002).

[30] L. Butov, A. Gossard, and D. Chemla, Macroscopically ordered state in an exciton system, Nature (London) **418**, 751 (2002).

[31] L. V. Butov and A. V. Kavokin, The behaviour of exciton–polaritons, Nat. Photon. **6**, 2 (2012).

[32] V. Negoita, D. W. Snoke, and K. Eberl, Huge density-dependent blueshift of indirect excitons in biased coupled quantum wells, Phys. Rev. B **61**, 2779 (2000).

[33] Z. Vörös, D. W. Snoke, L. Pfeiffer, and K. West, Direct measurement of exciton-exciton interaction energy, Phys. Rev. Lett. **103**, 016403 (2009).

[34] J. Wilkes and E. A. Muljarov, Dipolar polaritons in microcavity-embedded coupled quantum wells in electric and magnetic fields, Phys. Rev. B **94**, 125310 (2016).

[35] D. J. Choksy, C. Xu, M. M. Fogler, L. V. Butov, J. Norman, and A. C. Gossard, Attractive and repulsive dipolar interaction in bilayers of indirect excitons, Phys. Rev. B **103**, 045126 (2021).

[36] E. Blackwood, M. J. Snelling, R. T. Harley, S. R. Andrews, and C. T. B. Foxon, Exchange interaction of excitons in GaAs heterostructures, Phys. Rev. B **50**, 14246 (1994).

[37] C. Ciuti, V. Savona, C. Piermarocchi, A. Quattropani, and P. Schwendimann, Role of the exchange of carriers in elastic exciton-exciton scattering in quantum wells, Phys. Rev. B **58**, 7926 (1998).

[38] G. Ramon, A. Mann, and E. Cohen, Theory of neutral and charged exciton scattering with electrons in semiconductor quantum wells, Phys. Rev. B **67**, 045323 (2003).

[39] C. Schindler and R. Zimmermann, Analysis of the exciton-exciton interaction in semiconductor quantum wells, Phys. Rev. B **78**, 045313 (2008).

[40] M. M. Glazov, H. Ouerdane, L. Pilozzi, G. Malpuech, A. V. Kavokin, and A. D'Andrea, Polariton-polariton scattering in microcavities: A microscopic theory, Phys. Rev. B **80**, 155306 (2009).

[41] B. F. Gribakin, E. S. Khramtsov, A. V. Trifonov, and I. V. Ignatiev, Exciton-exciton and exciton–charge carrier interaction and exciton collisional broadening in GaAs/AlGaAs quantum wells, Phys. Rev. B **104**, 205302 (2021).

[42] J. A. Brum and G. Bastard, Electric-field-induced dissociation of excitons in semiconductor quantum wells, Phys. Rev. B **31**, 3893 (1985).

[43] J.-W. Wu and A. V. Nurmikko, Exciton-tunneling-lifetime enhancement by the Coulomb interaction in a quantum well with a perpendicular field, Phys. Rev. B **37**, 2711 (1988).

[44] O. L. Lazarenkova and A. N. Pikhtin, Energy spectrum of a nonideal quantum well in an electric field, Semiconductors **32**, 992 (1998).

[45] L. Schultheis, K. Kohler, and C. W. Tu, Energy shift and line broadening of three-dimensional excitons in electric fields, Phys. Rev. B **36**, 6609 (1987).

[46] S. I. Gubarev, O. V. Volkov, V. A. Koval'skii, D. V. Kulakovskii, and I. V. Kukushkin, Effect of screening by two-dimensional charge carriers on the binding energy of excitonic states in GaAs/AlGaAs quantum wells, J. Exp. Theor. Phys. Lett. **76**, 575 (2002).

[47] D. V. Kulakovskii, S. I. Gubarev, and Y. E. Lozovik, Screening of exciton states by quasi-two-dimensional electron gas in quantum wells, J. Exp. Theor. Phys. Lett. **74**, 118 (2001).

[48] A. L. C. Triques and J. A. Brum, Exciton center-of-mass dispersion in semiconductor quantum wells, Phys. Rev. B **56**, 2094 (1997).

[49] A. Siarkos, E. Runge, and R. Zimmermann, Center-of-mass properties of the exciton in quantum wells, Phys. Rev. B **61**, 10854 (2000).

[50] P. S. Grigoryev, I. V. Ignatiev, V. G. Davydov, Y. P. Efimov, S. A. Eliseev, V. A. Lovtcius, P. Y. Shapochkin, and M. Bayer, Exciton-light coupling in (In,Ga)As/GaAs quantum wells in a longitudinal magnetic field, Phys. Rev. B **96**, 155404 (2017).

[51] I. Vurgaftman, J. R. Meyer, and L. R. Ram-Mohan, Band parameters for III–V compound semiconductors and their alloys, J. Appl. Phys. **89**, 5815 (2001).

[52] B. Gerlach, J. Wusthoff, M. O. Dzero, and M. A. Smondyrev, Exciton binding energy in a quantum well, Phys. Rev. B **58**, 10568 (1998).

[53] M. A. Chukeev, E. Khramtsov, S. Zheng, I. V. Ignatiev, S. A. Eliseev, and Y. P. Efimov, Effect of electric field on excitons in a quantum well under additional optical excitation, Semiconductors **57**, 457 (2023).

[54] A. S. Kurdyubov, A. V. Trifonov, I. Y. Gerlovin, B. F. Gribakin, P. S. Grigoryev, A. V. Mikhailov, I. V. Ignatiev, Y. P. Efimov, S. A. Eliseev, V. A. Lovtcius, M. Assmann, M. Bayer, and A. V. Kavokin, Optical control of a dark exciton reservoir, Phys. Rev. B **104**, 035414 (2021).

[55] A. S. Kurdyubov, A. V. Trifonov, A. V. Mikhailov, Y. P. Efimov, S. A. Eliseev, V. A. Lovtcius, and I. V. Ignatiev, Nonlinear behavior of the nonradiative exciton reservoir in quantum wells, Phys. Rev. B **107**, 075302 (2023).